

Detection and Countermeasures for RF Unsafe Conditions for MR-conditional Devices

I. Graesslin¹, S. Weiss¹, E. Hassani¹, K. Nehrke¹, P. Vernickel¹, and S. Krueger¹

¹Philips Research Laboratories, Hamburg, Germany

Introduction The aging population causes an increasing demand for MR examinations in patients wearing implants. However, RF heating caused by coupling of conductive devices with the RF transmit coil represents a safety risk for the patient and the physician. Therefore, the presence of implants or interventional devices usually is a contra-indication for MR examinations. In addition to efforts on safe design of devices themselves, it may be advisable to monitor those devices during the scan. Previous work proposed to cancel planned scans if a reverse polarization pre-scan detected a device [1] or to terminate scans as soon as unsafe situations were detected by pick-up coils (PUC) [2,3]. This work has the objective to use the detection of unsafe events due to RF coupling to a device during an MR measurement to change the scan parameters of the parallel TX system rather than just terminating the scan. The aim is to re-establish a safe situation while trying to minimize image quality degradation. The proposed approach was evaluated in phantom as well as volunteer studies.

Methods A whole body 3T MRI system was used (Achieva, Philips Healthcare, the Netherlands) extended with eight parallel RF transmit channels [4] feeding an eight-channel body coil [5]. A real-time RF transmission monitoring system enabled the measurement of the complex currents in each of the eight RF transmit elements using one pick-up coil [6] per transmit element. The PUC signals are evaluated in real-time indicating, which transmit elements couple strongly with the device. These potentially dangerous elements are excluded from the imaging procedure as soon as the PUC signal(s) violate(s) a certain safety margin. To maintain optimal image quality, the RF shim setting is updated excluding the dangerous element(s). For the calculation of the RF shim coefficients, B1 maps are acquired at the beginning of the scan. To validate the concept, first phantom experiments were performed using a resonant wire coupling to the TX/RX body coil. For the phantom experiment, first, a B1 mapping and RF shimming experiment was performed with an oil-filled phantom of 40cm size. Then, a thin-insulated copper wire (diameter $D=150\mu\text{m}$, length $L=235\text{cm}$) was placed next to the phantom, and two small blocks of saline-based agar including fiber-optic probes for temperature measurement were placed at the wire ends (Luxtron790, LumaSense Technologies, Santa Clara, CA, USA). RF measurements confirmed that this set-up had a resonance frequency of 113MHz with a Q of 4. While the phantom was moved into the iso-center, PUC signals were acquired during RF transmission. Then, a high SAR scan (FFE, TR=160ms, TE=3.5ms, $\alpha=30^\circ$, whole body SAR=2W/kg) was applied for 25s, and RF heating due to MR-induced currents in the wire was monitored with an infra-red (IR) camera (VarioCam, Infratec, Dresden, Germany), while dielectric tip heating was simultaneously monitored by the fiber probes. The high SAR scan was repeated with various shim settings excluding RF elements, which showed amplitude changes in the PUC signals due to RF coupling, with the aim to reduce RF heating in the wire. B1 mapping was performed using an AFI (Actual Flip Angle Imaging) technique [7,8] (450x270x75mm³ FOV, 64x38x5 matrix, angle=60°, TR1=20ms, TR2=100ms, TE=2.3ms, transverse orientation). For RF shimming, magnitude least square fitting of the multi-coil maps was performed. Furthermore, the algorithm is capable of excluding channels from the optimization process. Finally, in vivo experiments were performed with a healthy volunteer, again starting with B1 mapping and RF shimming without wire. Then, the wire was added parallel to B_0 at a safe distance from the arm of the volunteer and separated by a foam spacer. For safety, only shim settings excl. elem. 7 were performed, which was closest to the wire and showed strongest coupling with the wire (c.f. last four shim sets in Tab. 1).

Results and Discussion When the oil phantom and the wire were moved into the bore, the PUC signal of channels 6&7 dropped by more than 10% (Fig. 1), which in our experience is a critical signal deviation for our system. Consequently, an RF shim set excluding channels 6&7 was activated as a countermeasure, indicated by a vast decrease of the respective PUC signals (see Fig. 1, $z_{\text{ch}6}=85\text{cm}/z_{\text{ch}7}=75\text{cm}$). Residual PUC signal is caused by currents induced by the remaining active elements. This cross-talk is possible because the wire disturbs the decoupling of all elements. Hence, the residual PUC signals correlate to the amount of coupling between the wire and de-activated elements. Monitoring these signals may be used to reactivate the element(s) as soon as a safe condition is re-established.

During the high SAR scan, the IR movies clearly depicted resistive RF heating occurring along the wire for the situation of no shimming (quadrature excitation) or RF shimming using all 8 channels (see Fig. 2). Heating was successfully suppressed (at the tip and along the cable) for the shim sets excluding transmission with element 7 (see Tab. 1). Obviously, imaging without one or more critical elements compromises image quality. However, the re-calculation of the RF shim sets for the remaining elements resulted in an acceptable quality, quantified by the coefficient of variation (CV) (see Tab. 1). Localized RF shimming could further improve the CV value.

For the in-vivo experiments, only the safe RF shim sets were used (excluding at least element 7). Tip heating was similar to the phantom experiments, which indicates that the approach is effective in-vivo. Images and B1 maps acquired using the adapted shim settings are shown in Fig. 3. In the phantom image, an artifact induced by the wire is clearly visible (due to coupling to the Rx element), while in the B1 maps only very minor artifacts are visible. The proposed concept could be applied e.g. for cardiac exams in patients with hip implants. It becomes even more effective for coils with more elements, e.g. z-segmented coils or local TX coil arrays. MR conditional devices are usually approved for a specific field strength. However, RF safety depends vastly on the specific transmit coil design. Therefore, the here proposed continuous monitoring of RF coupling to MR-conditional devices before and during scanning is advantageous to prevent unsafe situations for the patient.

Conclusion Real-time monitoring and control of RF currents in TX elements can be used to detect unsafe situations and to change RF transmission to reestablish a safe situation by switching off selected elements. The sensitivity of the method even allows monitoring coupling between already switched-off transmit elements and the device. This may be used to reactivate the element(s) as soon as a safe condition is re-established, e.g. induced by repositioning of an interv. device in the bore. The closer a device is located to a single/few transmit element(s) of a coil and the more transmit elements exist the easier it is possible to drastically reduce RF coupling to that/those element(s) while maintaining an acceptable image quality. This method may further increase the safety of MR-conditional devices and allow more freedom in their use.

Acknowledgements We would like to thank R. Luechinger, Universitaetsspital, MR-Zentrum VMR30, Zuerich for support and helpful discussions.

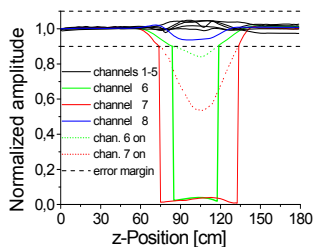


Fig. 1: Normalized amplitude of PUC signals over z-position. Detection of unsafe “wire condition” and switching off channel #6 and #7.

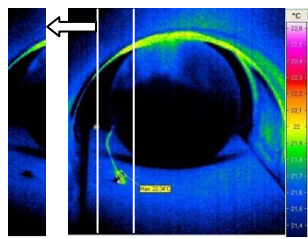


Fig. 2: IR picture of experimental setup and heated wire (left). Wire with channel 7 turned off no heating is visible (left).

RF shim type	$\Delta T_{\text{max}} [\text{K}] @\text{tip}$	$\Delta T_{\text{max}} [\text{K}] @\text{IR}$	CV
quad. Excit.	14K	0.7	10.43%
all channels	7K	0.33	3.20%
/wo chan. 7	0.7K	0.1	7.35%
/wo chan. 6,7	0.5K	0.06	8.66%
/wo chan. 7,8	0.3K	0.03	32.90%
/wo chan. 6,7,8	0.2K	0.02	44.09%

Tab. 1: Maximum RF heating measured by fiber probe at tip in agar block and by IR camera along the wire.

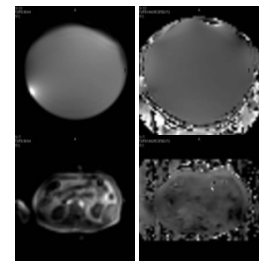


Fig. 3: Images (left) and B1 maps (right) acquired with adapted shim settings for phantom (top) and volunteer (bottom).

References

- [1] Overall WR. et al. [2010] MRM 64(3):823–833
- [2] Krueger S. et al. [2008] ISMRM 16:896
- [4] Graesslin I. et al. [2006] ISMRM 14:129
- [5] Graesslin I. et al. [2007] ISMRM 15:1086
- [7] Yarnykh VL. [2007] MRM 57(1):192-200
- [8] Nehrke K. et al. [2009] MRM 61(1):84-92
- [3] Graesslin, I. et al. [2008] ISMRM Safety WS #40
- [6] Vernickel P. et al. [2007] MRM 58(2):381-9